Cerebral Cortex June 2012;22:1455–1454
doi:10.1093/cercor/bhr230
Advance Access publication August 1, 2011

Laterality Patterns of Brain Functional Connectivity: Gender Effects

Dardo Tomasi[1] and Nora D. Volkow[1,2]

[1]National Institute on Alcohol Abuse and Alcoholism and [2]National Institute on Drug Abuse, Bethesda, MD 20892, USA

Address correspondence to Dr Dardo Tomasi, Laboratory of Neuroimaging (LNI/NIAAA), Medical Department, Building 490, Brookhaven National Laboratory, 30 Bell Avenue, Upton, NY 11973, USA. Email: tomasi@bnl.gov.

Lateralization of brain connectivity may be essential for normal brain function and may be sexually dimorphic. Here, we study the laterality patterns of short-range (implicated in functional specialization) and long-range (implicated in functional integration) connectivity and the gender effects on these laterality patterns. Parallel computing was used to quantify short- and long-range functional connectivity densities in 913 healthy subjects. Short-range connectivity was rightward lateralized and most asymmetrical in areas around the lateral sulcus, whereas long-range connectivity was rightward lateralized in lateral sulcus and leftward lateralizated in inferior prefrontal cortex and angular gyrus. The posterior inferior occipital cortex was leftward lateralized (short- and long-range connectivity). Males had greater rightward lateralization of brain connectivity in superior temporal (short- and long-range), inferior frontal, and inferior occipital cortices (short-range), whereas females had greater leftward lateralization of long-range connectivity in the inferior frontal cortex. The greater lateralization of the male's brain (rightward and predominantly short-range) may underlie their greater vulnerability to disorders with disrupted brain asymmetries (schizophrenia, autism).

Keywords: connectivity, functional connectomes, laterality

Introduction

Brain anatomy and function differ for the left and right hemispheres of the human brain, which is believed to reflect not only the emergence of language but also developmental and genetic factors (Toga and Thompson 2003). Brain asymmetry is present at the structural level in the fetal brain in humans and nonhuman primates (Galaburda et al. 1978) and appears to be disrupted in patients with autism spectrum disorder (ASD), schizophrenia, and developmental dyslexia (Saugstad 1999).

Brain laterality differences between the genders have also been documented and may underlie gender differences in cognitive styles (Proust-Lima et al. 2008). For example, the females' overall linguistic advantage over males may reflect stronger leftward lateralization of the language networks, whereas the males' spatial skills advantage over females may reflect stronger rightward lateralization of visuospatial networks (Clements et al. 2006). Gender differences in the lateralization of brain function might also contribute to gender differences in the incidence of neurospychiatric disorders such as ASD (Baron-Cohen et al. 2005) and schizophrenia (Narr et al. 2001). However, the gender differences in the lateralization of brain function are still controversial, and few studies have been done to address it. For example, whereas some blood oxygen level–dependent-functional magnetic resonance imaging studies have suggested that lateralization of language might be more pronounced in males than in females (Shaywitz et al. 1995) others have failed to reproduce these gender effects (Frost et al. 1999).

Intrinsic brain activity captured during brief (5–10 min) magnetic resonance imaging (MRI) scanning during resting conditions (Biswal et al. 1996; Biswal et al. 2010) can now be used to evaluate local and distant functional connectivity (Sepulcre et al. 2010), including the assessment of functional brain asymmetry (Liu et al. 2009) in the male and in the female brain. Studies based on 200 seed regions of interest (ROIs) distributed uniformly in the brain reported a small but significant gender by laterality interaction effect on the strength of the functional connectivity (stronger in males than in females) between seed regions (Liu et al. 2009). However, the asymmetry of short- or long-range functional connections and their interactions with gender have not been evaluated.

Recently, we proposed *functional connectivity density mapping* (FCDM), a voxelwise data-driven technique to assess the short-range (local) functional connectivity density (*l*FCD) (Tomasi and Volkow 2010). Here, we describe a novel method based on FCDM and a standard graph theory approach to separately assess short- and long-range FCD, which we used to map the laterality patterns of functional connectivity and to evaluate gender effects in 913 subjects from a large public MRI database (Biswal et al. 2010). A simple parallel computing method was used to speed up significantly (1000 times faster) the overwhelming computation of graph theory measures of *global functional connectivity density* (*g*FCD) at 3-mm isotropic spatial resolution. Based on documented anatomical and functional rightward asymmetries (Devlin et al. 2003; Toga and Thompson 2003; Schönwiesner et al. 2007; Okamoto et al. 2009), we hypothesized that temporal and cingulate cortices would show a rightward lateralization for both short- and long-range FCD. We also predicted that the laterality of the short- and long-range FCD patterns would show significant gender effects in a regional specific manner.

Materials and Methods

Subjects

Functional scans that were collected in "resting-state" conditions and correspond to 913 healthy subjects (Table 1) from 19 research sites of the "1000 Functional Connectomes" Project (http://www.nitrc.org/projects/fcon_1000/) were included in the study. Data sets from other research sites that were not available at the time of the study (pending verification of IRB status) did not report demographic variables (gender and age), exhibited image artifacts that prevented the study of short- and long-range FCD, or did not meet the imaging acquisition criteria (3 s $\geq$ repetition time, full brain coverage, time points > 100, spatial resolution better than 4 mm) were not included in the study.

Image Preprocessing

The statistical parametric mapping package SPM2 (Wellcome Trust Centre for Neuroimaging, London, UK) was used for image realignment

Table 1

Demographic data corresponding to 408 males (M) and 505 females (F) and imaging parameters (Tp: time points and TR: repetition time) for all 913 data sets from 19 research sites

Data set	Subjects	Age (years)	Tp	TR (s)
Ann Arbor	21M/2F	13–41	295	1.0
Bangor	20M/0F	19–38	265	2.0
Beijing	75M/122F	18–26	225	2.0
Berlin	13M/13F	23–44	195	2.3
Cambridge	75M/123F	18–30	119	3.0
Cleveland	11M/20F	24–60	127	2.8
Dallas	12M/12F	20–71	115	2.0
ICBM	17M/25F	19–85	128	2.0
Leiden	23M/8F	20–27	215	2.2
Leipzig	16M/21F	20–42	195	2.3
MIT	17M/18F	20–32	145	2.0
Newark	9M/10F	21–39	135	2.0
New York	8M/12F	18–46	175	2.0
Orangeburg	15M/5F	20–55	165	2.0
Oulu	37M/65F	20–23	245	1.8
Oxford	12M/10F	20–35	175	2.0
Palo Alto	2M/15F	22–46	235	2.0
Queensland	11M/7F	21–34	190	2.1
Saint Louis	14M/17F	21–29	127	2.5

Note: ICBM, International Consortium for Brain Mapping; MIT, Massachusetts Institute of Technology.

and spatial normalization to the stereotactic space of the Montreal Neurological Institute (MNI) using a 12-parameter affine transformation with medium regularization, 16-nonlinear iterations, voxel size of 3 × 3 × 3 mm^3. Other preprocessing steps were carried out using IDL (ITT Visual Information Solutions, Boulder, CO). A multilinear regression approach that used the time-varying realignment parameters (3 translations and 3 rotations) was applied to minimize motion related fluctuations in the MRI signals (Tomasi and Volkow 2010), and the global signal intensity was normalized across time points. Band-pass temporal filtering (0.01–0.10 Hz) was used to remove magnetic field drifts of the scanner (Foerster et al. 2005) and minimize physiologic noise of high frequency components (Cordes et al. 2001). Voxels with signal-to-noise (as a function of time) < 50 were eliminated to minimize unwanted effects from susceptibility-related signal-loss artifacts on FCDM. MRI time series reflecting the preprocessing steps were saved in hard drive for subsequent analyses.

Local and Global FCD

The preprocessed image time series underwent FCDM to compute the strength of the *l*FCD (Tomasi and Volkow 2010). The number of *local* connections at every voxel location x_0, $k(x_0)$, was determined through Pearson correlations between time-varying signals at x_0 and those from its closest neighbors using an arbitrary threshold $R > 0.6$ (Tomasi and Volkow 2010, 2011a, 2011b, 2011c, 2011d). This correlation threshold was selected in our previous work because $R < 0.4$ increased false positive rate and CPU time and $R > 0.7$ lead to *l*FCD maps with reduced dynamic range and lower sensitivity; thus we fixed $R = 0.6$ for all calculations (Tomasi and Volkow 2010). In addition, standard graph theory (degree centrality) was used to map the strength of the *g*FCD from the preprocessed image time series (Tomasi and Volkow 2011c) (for a complete collection of graph theory measures, see Rubinov and Sporns 2010). Two voxels were considered functionally connected if the Pearson linear correlation factor $R > 0.6$; we selected this correlation threshold to be consistent with that used to compute the *l*FCD maps. We verified that the rescaled *g*FCD (normalized to its mean value in the whole brain) was stable under threshold variations in the range $0.5 < R < 0.7$. The *g*FCD at a given voxel x_0 was computed as the *global* number of functional connections, $k(x_0)$, between x_0 and all other $N - 1 = 57\,712$ voxels in the brain. This calculation was repeated for all x_0 voxels in the brain and involved the computation of a N^2 correlation matrix.

Parallel Computing

A simple approach based on data parallelism was implemented to speed up the calculation of the *g*FCD by taking advantage of multiprocessor computer architectures. Specifically, the data was distributed across processing nodes in a way that all nodes executed the same code (gFCD.exe; 32 bit) on different imaging data (1 gFCD.exe per subject, 2 subjects per core). The standalone gFCD.exe code (188 kB) efficiently allocated 128 MB of dynamic memory via pointer reference by setting the handler mode for malloc, a standard C subroutine for fast operations on random-access memory. The gFCD.c code was developed and compiled using Visual C++ 6.0 (Microsoft Corp, Redmond, WA). Thus, the computation of the *g*FCD maps required only 120 min/subject (single core PC without Hyper-Threading Technology [HTT]), which was significantly faster than what could be achieved using user-friendly high-level programing languages such as IDL or Matlab (~few days per subject).

A workstation with 2 Intel Xeon X5680 processors (6 cores per processor, 12 MB L3 Cache, 64-bit, 3.33 GHz), which accounted a total of 12 cores and allows 24 processing threads with HTT, running Windows 7 (64-bit) was used to compute the *g*FCD maps for each subject. Note that HTT enabled the operating system to address 2 virtual processors for each of the 12 cores that were physically present. Twenty-four batches of jobs (gFCD.exe) were submitted simultaneously by terminal commands; Windows 7 distributed the workflow among the 24 virtual processors. Thus, our simple but efficient parallelization approach allowed us to compute 24 subjects (1 subject per virtual processor) at once and required in average only 5 min/subject to complete.

Short- and Long-Range FCD

The *l*FCD included all voxels that belonged to the local cluster of functionally connected voxels. Since it predominantly reflects the regional short-range functional connectivity, we defined: *short-range* FCD = *l*FCD. Since the *g*FCD included both local and distal connections, we defined *long-range* FCD = *g*FCD – *l*FCD (Tomasi and Volkow 2011a). These maps inherited the radiological convention (left is right) of the native images. Short- and long-range FCD maps were spatially smoothed (8 mm) in SPM to minimize the differences in the functional anatomy of the brain across subjects.

Laterality Index

We developed a voxelwise method to compute the laterality of the brain's functional connectivity that contrasts FCD measures at homologous voxels in the left and right hemispheres. For this purpose, short- and long-range FCD maps with neurological convention (R: right is right) were additionally created by flipping (as mirror reversal of) the radiological FCD maps (L) across the *x*-axis. Then, the strength and direction of the short- and long-range FCD asymmetries were mapped voxel-by-voxel by using a laterality index (LI) (Steinmetz 1996):

$$LI = (R - L)/(R + L),$$

which partially accounts for intersubject variability and differential acquisition protocols among research sites. Negative LI values indicate leftward asymmetry and positive LI values indicate rightward asymmetry. The Fisher transform was used to normalize the step distributed LI values. Short- and long-range LI maps were spatially smoothed (8 mm) to minimize the differences in the functional anatomy of the brain across subjects. Group analyses of these LI maps were carried out in SPM using a 2-way analysis of variance (ANOVA) model with 2 conditions (short- and long-range FCD), 2 groups (males and females), and 1 covariate (age). Voxels with a conservative $P_{FWE} < 0.05$, corrected for multiple comparisons in the whole brain with a family-wise error (FWE) correction at the voxel-level were considered statistically significant across subjects. The population-average landmark- and surface-based atlas of the cerebral cortex (Van Essen 2005) provided in the installation package of the MRIcron image viewer (http://www.nitrc.org/projects/mricron) was used to identify FCD clusters with Brodmann areas (BAs) in the stereotactic space of the MNI.

Volume-of-Interest Analyses

Isotropic cubic masks containing 27 imaging voxels (0.73 mL) were defined at the coordinates of the cluster centers in the right hemisphere (Table 2) and their homologous regions in the left hemisphere to extract the average strength of the laterality of the short- and long-range FCD from individual LI maps and using a custom program written in IDL. The volume-of-interest (VOI) measures were used to assess the significance of the laterality findings as well as that of gender (assessed with parametric *t*-test and nonparametric Kolmogorov–Smirnov and Mann–Whitney–Wilcoxon tests) effects in Statview (SAS Institute Inc., Cary, NC) and Microcal Origin (Microcal Software Inc., Northampton, MA).

Results

Short- and Long-Range Functional Connectivity

The average distribution of the short-range FCD was maximal in posterior cingulate and ventral precuneus (Fig. 1*A*). Other regions with high amplitude of short-range FCD included ventral occipital (cuneus), posterior lateral parietal (angular gyrus), and ventral and dorsolateral prefrontal cortices. The average distribution of the long-range FCD was maximal in the visual cortex, followed by posterior cingulate and ventral precuneus (Fig. 1*B*). Angular gyrus, superior and inferior parietal, and dorsolateral prefrontal and temporal cortices also had significant long-range FCD. Note that the patterns of these highly connected regions (both short- and long-range) had a similar distribution in the left and in the right hemisphere. Overall, the short- and long-range FCD were lower for subcortical than for cortical regions.

Laterality Index

The statistical analysis of the LI patterns across all 913 subjects revealed that the short-range FCD was predominantly right lateralized and, except for the angular gyrus, included regions with low FCD. Regions showing a rightward asymmetry in short-range FCD were located in the vicinities of the lateral sulcus, including superior and middle temporal gyri (BAs 21, 22, 40, 41, and 42) and in the postcentral gyrus (BA 3). Smaller regions in prefrontal cortex (BAs 6, 11, and 47), insula (BA 13), and temporal pole (BAs 20 and 38) also exhibited rightward asymmetry. Regions showing a leftward asymmetry in short-range FCD were restricted and included small areas in the posterior cingulate (BA 29), inferior posterior (BA 17) and superior occipital cortex (BA 19), frontoparietal cortices (BAs 6 and 8), angular gyrus (BA 19/39), and hippocampus (Fig. 2*A* and Table 2). Temporal and inferior posterior occipital cortices showed the largest short-range laterality effects (LI = 22.1 ± 0.6% and –16.8 ± 0.6%, respectively; mean ± standard error).

As for the short-range FCD, the long-range FCD was predominantly right lateralized around the lateral sulcus (LI = 17.8 ± 0.7%) and left lateralized in the inferior posterior occipital cortex (LI = –12.7 ± 0.5%; Fig. 2*B* and Table 2) but also showed strong rightward lateralization in anterior and dorsal cingulate cortex (including BAs 23, 24, 31, and 32) and strong leftward lateralization in the frontal cortex (Broca's area, which encompasses pars opercularis, BA 44; pars transversalis, BA 45; and pars orbitalis, BA 47) and in the angular gyrus (BA 19/39). Comparisons of the laterality pattern for short- versus long-range FCD showed an opposite pattern in inferior orbital frontal cortex (pars orbitalis; BA 47) that showed leftward laterality in long-range FCD but rightward laterality for short-range FCD (Table 2).

Volumes of Interests

The VOI analysis of short- and long-range FCD in homologous regions of the left and right hemispheres (Fig. 3) revealed that caudate had the strongest rightward lateralization both for

Table 2

Statistical significance (*T*-score) of the LI in 3-mm isotropic (cubic) ROIs centered at the MNI coordinates that show rightward (positive % mean ± SE) or leftward (negative % mean ± SE) lateralization of short- or long-range FCD

Brain region	BA nucleus	MNI			Lateralization		
		x (mm)	*y* (mm)	*z* (mm)	Short-range *T*-score (%)	Long-range *T*-score (%)	Short > long *T*-score
Post cingulate	29	3	−42	6	−13.4 (−10.4 ± 0.5)	−6.5 (−6.3 ± 0.4)	−3.5
Calcarine	17	3	−102	12	−11.6 (−16.8 ± 0.6)	−7.4 (−12.7 ± 0.5)	NS
Lingual	17	3	−57	6	−7.2 (−8.0 ± 0.7)	−6.3 (−8.7 ± 0.7)	NS
Hippocampus	37	30	−42	0	−5.6 (−5.8 ± 0.5)	−7.1 (−9.1 ± 0.6)	NS
Superior frontal	8	15	30	57	−4.3 (−4.9 ± 0.7)	−9.8 (−14.2 ± 0.9)	4.9
Hippocampus	37	36	−39	−6	−4.1 (−4.4 ± 0.5)	−6.1 (−7.9 ± 0.6)	NS
Angular	19/39	42	−72	36	−3.8 (−5.0 ± 1.0)	−12.9 (−19 ± 1.2)	7.6
Sup motor area	6	12	18	66	−3.1 (−4.9 ± 0.6)	−4.3 (−7.7 ± 0.8)	NS
Superior occipital	19	24	−78	39	−2.6 (−3.5 ± 1.0)	−9.7 (−14.7 ± 1.3)	5.8
Inferior frontal triangle	45	51	27	18	NS (−2.2 ± 1.0)	−18.2 (−25.6 ± 1.2)	13.1
Precentral	9	45	15	51	NS (0.1 ± 0.6)	−9.3 (−11.4 ± 0.8)	7.2
Middle frontal	6	51	12	45	NS (1.4 ± 0.6)	−8.4 (−10.9 ± 0.8)	7.4
Superior frontal	9	15	51	39	NS (−2.4 ± 0.7)	−7.4 (−11.1 ± 1.0)	4.7
Caudate		9	6	12	NS (1.2 ± 0.5)	6.2 (7.4 ± 0.5)	−4.2
Thalamus	Pulvinar	15	−30	6	NS (0.4 ± 0.8)	8.5 (10.7 ± 0.9)	−6.5
Insula	13	30	30	6	2.9 (3.0 ± 0.2)	3.4 (4.2 ± 0.2)	NS
Hippocampus	20	33	−21	−12	3.4 (3.8 ± 0.8)	9.3 (12.3 ± 1.1)	−5.0
Inferior orbital frontal	47	45	36	−9	4.4 (5.0 ± 1.0)	−9.3 (−14.7 ± 1.3)	9.9
Postcentral	3	36	−30	42	4.4 (2.4 ± 0.2)	6.2 (4.3 ± 0.3)	NS
Cingulate	23	3	−24	36	5.7 (5.6 ± 0.6)	12.9 (13.6 ± 0.6)	−6.4
Medial frontal	6	3	6	51	5.7 (5.7 ± 0.6)	12.4 (15.0 ± 0.7)	−6.0
Precuneus	23	15	−66	33	9.3 (11.2 ± 0.9)	9.2 (13.6 ± 1.2)	NS
Temporal pole	38	63	6	−3	13 (20.7 ± 0.5)	7.1 (14.8 ± 0.5)	2.7
Superior temporal	22	69	−24	12	14.4 (22.1 ± 0.7)	9.1 (17.8 ± 0.7)	NS
Mid orbital frontal	11	27	45	−18	15.3 (16.8 ± 1.0)	12.2 (16.3 ± 1.0)	NS
Temporal pole	38	57	15	−9	22.6 (21.6 ± 0.6)	12.8 (15.0 ± 0.6)	4.4

Note: SE, standard error; NS, not significant.

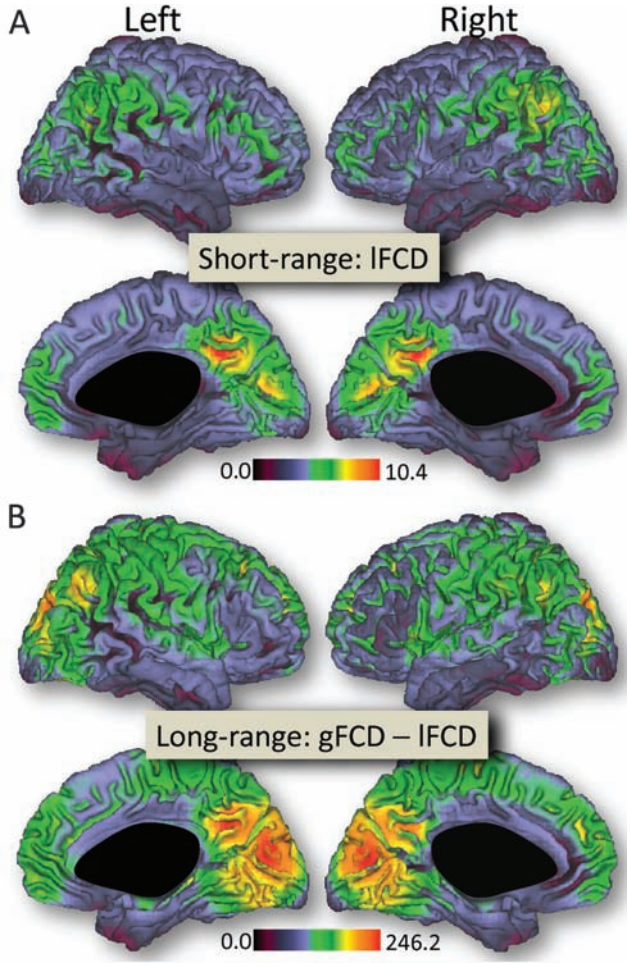

Figure 1. Surface rendering showing the distribution of short-range (*A*) and long-range (*B*) FCD in the human brain. Sample: all 913 subjects included. Threshold used to compute short- and long-range FCD: R > 0.6. The images were created using the Computerized Anatomical Reconstruction and Editing Toolkit (CARET) 5.0, which is freeware software developed at Washington University (http://brainvis.wustl.edu/wiki/index.php/Caret:About).

short-range (22.2 ± 1.3%) and long-range (37.8 ± 2.5%) FCD and that temporal pole, superior temporal, and middle orbital frontal gyri also showed strong rightward lateralization for both short- and long-range FCD (>7.3%). The rightward lateralization in cingulate cortex and thalamus was strong for long-range FCD (>7.3%) but much weaker for short-range FCD (<3.7%). The strongest leftward lateralization occurred at the middle frontal gyrus, both for short-range (–30.5 ± 1.8%) and long-range (–11.9 ± 0.6%) FCD; the calcarine and posterior cingulate cortices, pars inferior frontal triangularis, and supplementary motor area also showed strong leftward lateralization for both short- and long-range FCD. The leftward lateralization in angular gyrus was strong for long-range FCD (–18.8 ± 1.1%) but much weaker for short-range FCD (–3.5 ± 0.2%). The inferior orbital frontal (pars orbitalis) exhibited strong leftward lateralization of long-range FCD (–15.0 ± 0.8%) and weak rightward lateralization of short-range FCD (1.1 ± 0.1%).

Gender

The group analysis revealed significant gender effects in the laterality of FCD (Fig. 4), although these were limited to small brain regions. The short-range FCD revealed significantly greater laterality in males (N = 408) than females (N = 505). This included higher rightward lateralization on short-range connectivity in inferior frontal (pars orbitalis, triangularis, and opercularis) and superior temporal and inferior parietal (postcentral gyrus) cortices (Fig. 4 and Table 3). The long-range connectivity in males showed higher rightward lateralization in superior temporal cortex, whereas females showed greater leftward lateralization of long-range connectivity in the inferior frontal cortex areas where males showed higher rightward lateralization for short-range connectivity (Fig. 4 and Table 3).

Discussion

Regions with high functional connectivity may play an important role for the optimal efficiency and integration of functional networks both at rest and during task conditions (Biswal et al. 1995; Tomasi and Volkow 2011b) and could be critical to minimize the number of steps to connect any pair of neurons (Bassett and Bullmore 2006; Bullmore and Sporns 2009). An unbalance between short- and long-range FCD might result in pathology, as suggested by studies in patients with ASD who showed increased short-range and reduced long-range connectivity (Anderson et al. 2011; Barttfeld et al. 2011).

In this study, we evaluate for the first time the laterality patterns that emerge from resting-state functional connectivity data sets, separately for short- and for long-range FCD, and assess the gender effects on these patterns at an unmatched spatial resolution (3-mm isotropic). The main findings of the study are: 1) in resting conditions, the FCD was right lateralized in precuneus, superior parietal, temporal, and middle frontal cortices (short- and long-range) and in inferior orbital frontal (short-range) and cingulate (long-range) cortices and left lateralized in posterior occipital, superior frontal, lateral parietal, and posterior cingulate cortices (short- and long-range) and in the inferior frontal cortex (long-range) and 2) males had greater rightward laterality of brain connectivity in superior temporal, inferior frontal, and inferior occipital cortices (short-range) and in the superior temporal cortex (long-range) than females, whereas females showed greater leftward lateralization of long-range connectivity in inferior frontal cortex.

Laterality

The voxelwise analysis revealed a rightward lateralization of the short- and long-range FCD in a large region of the temporal cortex (including superior and medial temporal gyri) and in inferior frontal gyri that to our knowledge had not been previously reported. The rightward lateralization likely reflects interhemispheric differences in the anatomy of the temporal cortices such as the larger extend of the Silvian fissure (which bordered the area that on our analyses showed the largest rightward laterality) on the right hemisphere than on the left (LeMay and Kido 1978; Kertesz et al. 1986). However, this lateralization pattern could also reflect in part the high levels of acoustic noise emitted by the MRI scanner during echo planar imaging acquisition (Tomasi et al. 2005) since sound processing (Devlin et al. 2003; Schönwiesner et al. 2007; Okamoto et al. 2009), including auditory motion perception is right lateralized (Hirnstein et al. 2007), which is likely to have enhanced brain activity predominantly in the right temporal cortex. Abnormal

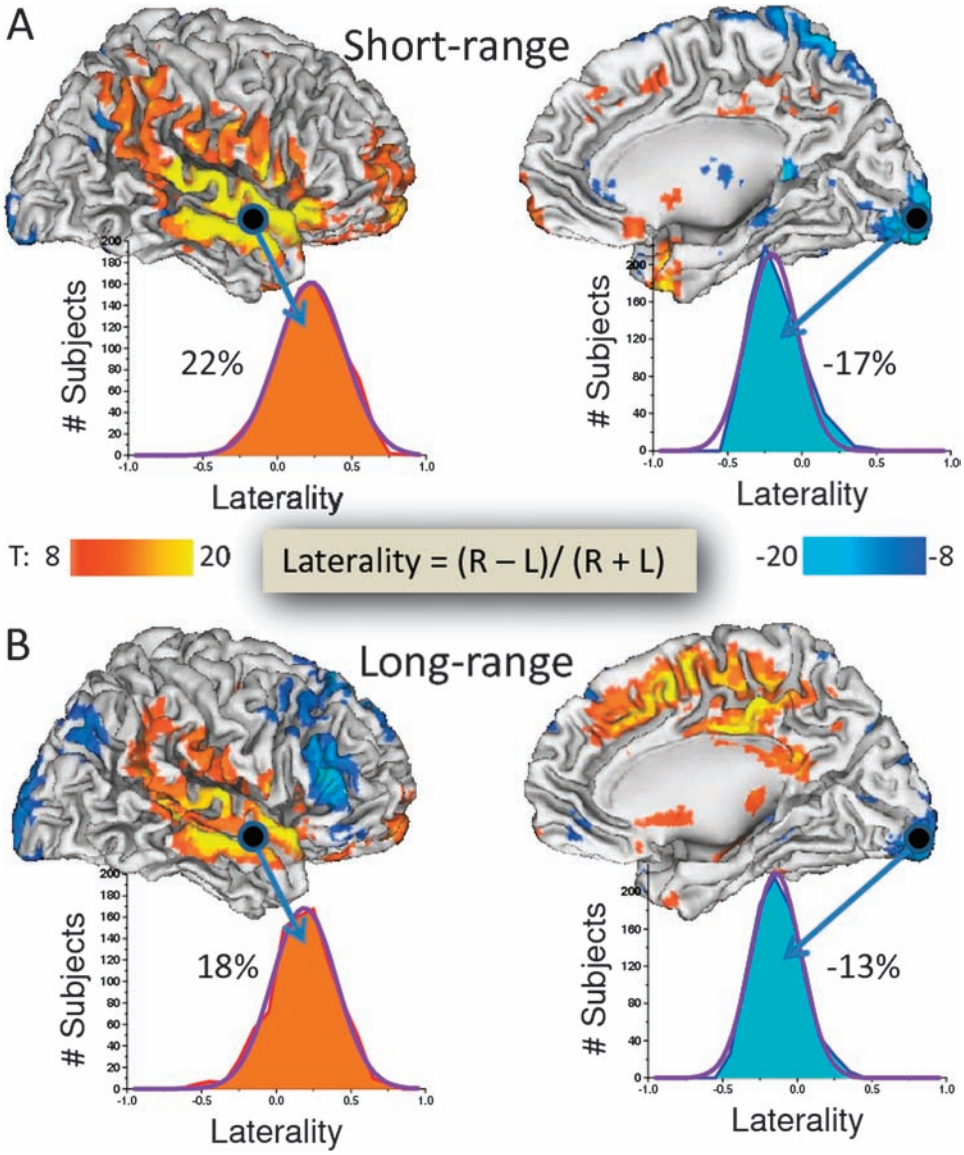

Figure 2. Statistical significance of the LI (inserted formula) corresponding to short- (A) and long-range (B) FCD in the left (L) and right (R) hemispheres. Color patterns (*T*-scores) highlight the statistical significance of rightward (red–yellow) and leftward (blue–cyan) asymmetries. Statistical analyses: 1-way ANOVA. Histograms reflect the LI probability distribution across subjects and exemplify the relative percent FCD asymmetry in temporal (Heschl's gyrus) and occipital (posterior petalia) cortices. Sample: 913 subjects.

hemispheric asymmetries particularly in the Heschl's gyrus (auditory cortex) were associated with auditory hallucinations (Chance et al. 2008) and those in frontal areas have been implicated in schizophrenia (Bear et al. 1986; Chance et al. 2005).

The rightward asymmetry of the long-range FCD in cingulate cortex is consistent with prior studies reporting higher resting functional connectivity of the right cingulate cortex with prefrontal and parietal cortices than the left (Yan et al. 2009). The lateralization in cingulate cortex is also consistent with the structural asymmetries reported for the cingulate (Huster et al. 2007) and paracingulate cortices (Paus et al. 1996). Rightward lateralization of the cingulate cortex was more pronounced for females than for males and may be clinically significant since loss of the asymmetry in the anterior cingulate cortex was reported in female patients with schizophrenia (Takahashi et al. 2002). Our findings did not corroborate the rightward asymmetry of the functional connectivity strength in occipital–parietal cortices and insula previously reported in young adults using an ROI approach that did not distinguish between short- and long-range connections (Liu et al. 2009). However, methodological differences between studies might account for this discrepancy. Specifically, the LI used by Liu et al. contrasted the strength of the differential ipsilateral versus contralateral functional connectivity between hemispheres using 200 arbitrary ROI in each hemisphere. The present study is based on a larger sample and used a voxelwise and data-driven approach with a simple LI that reflects differences in connectivity density between hemispheres.

The leftward lateralization of short- and long-range FCD in posterior occipital cortex likely reflects the occipital petalia (LeMay 1976), a protrusion of the left hemisphere relative to the right (Toga and Thompson 2003). The leftward asymmetry of the long-range FCD in inferior prefrontal cortex and angular

gyrus is consistent with previous resting-state studies on functional connectivity (Liu et al. 2009). The leftward lateralization is also likely to reflect the lateralization of language to the left hemisphere. Though traditionally, language production has been associated to Broca's area (BAs 44 and 45), a premotor area in BA 6 that controls complex articulations is also implicated (Price 2010). Similarly, language comprehension that is ascribed to Wernicke's area (predominantly includes posterior BA 22) also encompasses BAs 20, 21, 38, and 39 (Price 2010). Morphological studies have shown the leftward asymmetry of Broca's area and of the planum temporale (adjacent to angular gyrus) in humans (Falzi et al. 1982; Steinmetz 1996; Amunts et al. 1999) and nonhumans

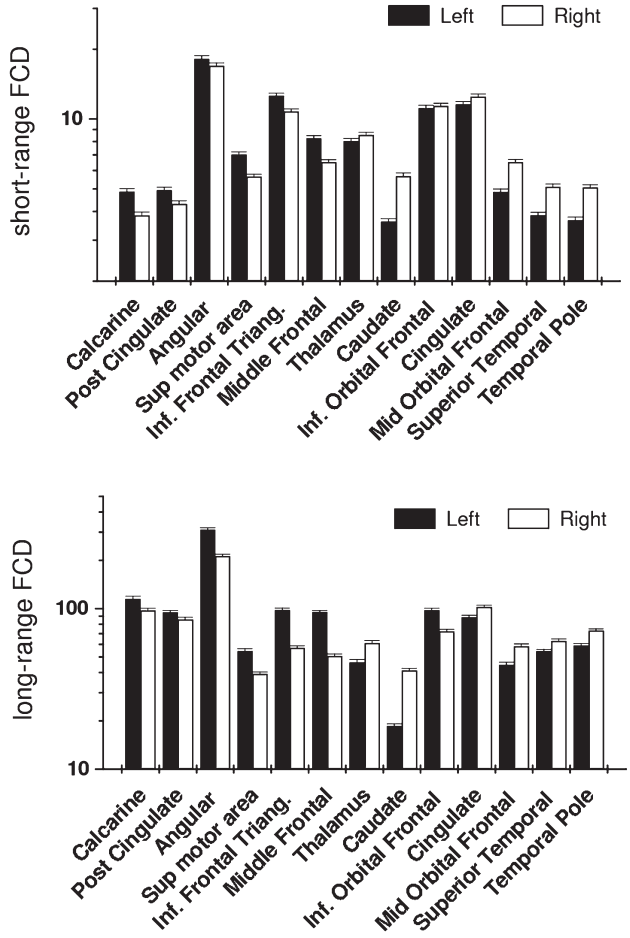

Figure 3. Average number of functional connections with local (short-range FCD) and distal (long-range FCD) voxels for different VOIs showing significant lateralization in SPM analyses (Table 2). Measures include VOIs in the right hemisphere and their homologous VOIs in the left hemisphere. For all regions except inferior orbital frontal (short-range; not significant, NS), statistical significance for left–right differences in short- and long-range FCD: $P < 0.001$. Bars reflect standard errors. Sample: 913 subjects. Threshold used to compute short- and long-range FCD: $R > 0.6$.

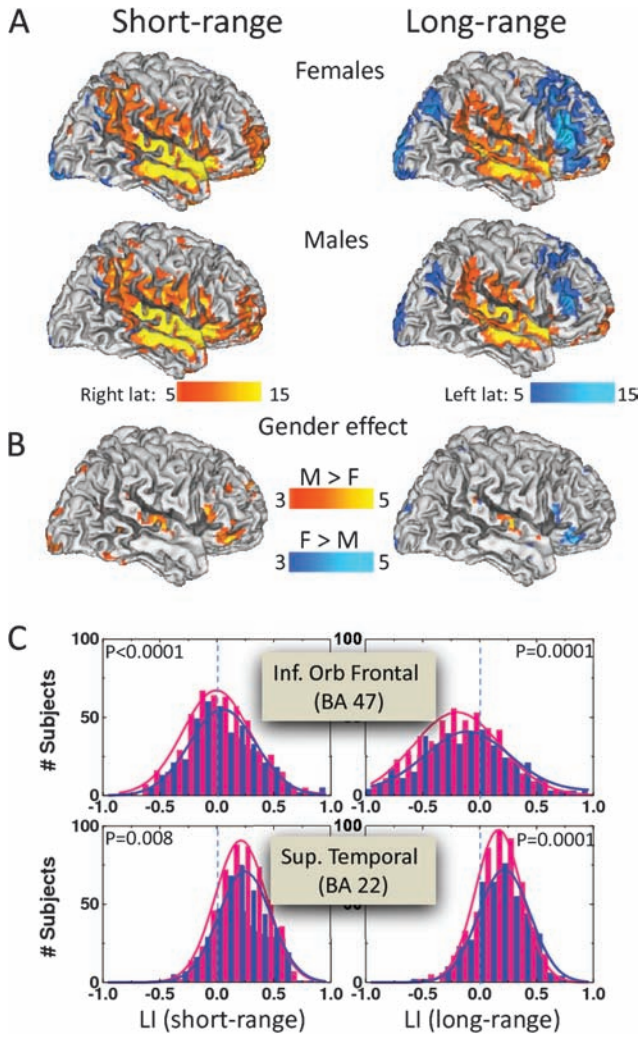

Figure 4. Statistical significance of the LI corresponding to short- (left panels) and long-range (right panels) FCD for females and males (*A*) and for the differences between genders (*B*). Color maps (*T*-score) indicate brain regions with significant rightward (red–yellow) or leftward (blue–cyan) lateralization for males (M) and females (F) or regions where LI significantly differed between males and females. Statistical analysis: 1-way ANOVA. (*C*): LI distributions corresponding to short- (left panels) and long-range (right panels) FCD for males (blue) and females (pink) in 4 different VOIs in dorsolateral prefrontal and cingulate cortices. Solid lines are Gaussian fits. Sample: 505 healthy females and 408 healthy males.

Table 3
Statistical significance (*T*-score) of gender effects on laterality of short- and long-range FCD in 3-mm isotropic (cubic) ROIs centered at the peak coordinates (*x*, *y*, *z*) of statistically significant clusters

Brain region	*K* voxels	BA	MNI			LI		
			x (mm)	*y* (mm)	*z* (mm)	Females short (long)	Males short (long)	Females > males short (long)
Pars orbitalis	270	47	54	33	−6	2.9 (−5.2)	6.3 (NS)	−2.8 (−3.6)
Pars triangularis		45	57	27	3	NS (−4.7)	3.6 (NS)	−2.1 (−2.2)
Pars opercularis		44	60	21	18	NS (−4.9)	4.0 (NS)	−2.1 (−2.2)
Superior temporal	294	22	66	−9	3	10.5 (6.0)	12.2 (9.5)	−2.3 (−2.9)
Postcentral		43	66	−15	30	6.7 (4.3)	7.7 (7.2)	NS (−2.4)
Superior temporal		22	66	−24	12	13.2 (7.7)	14.5 (11.2)	−2.3 (−3.1)

Note: Sample: 505 healthy females and 408 healthy males. *K*, cluster size.

primates (Yeni-Komshian and Benson 1976), and abnormalities in the leftward asymmetry of language areas have been implicated in developmental dyslexia (Hynd et al. 1990; Larsen et al. 1990; Galaburda 1995) and schizophrenia (Crow et al. 1989; Bilder et al. 1999; Narr et al. 2001).

Short- versus Long-Range Laterality

There were significant laterality differences between short- and long-range FCD. Most notable, a leftward lateralization was observed for the long-range but not for the short-range FCD in inferior frontal cortex and angular gyrus. Similarly, an opposite laterality pattern was observed in posterior cingulate (BA 29) and thalamus (pulvinar) for the short-range (leftward) versus the long-range (rightward) FCD. The functional significance of these laterality differences is unclear. However, since long-range cortical connections are implicated in functional integration (Bressler 1995) and local connections are implicated in functional specialization (Schroeder and Lakatos 2009), we speculate that differences in asymmetry between long- and short-range FCD could reflect differences in integration and specialization between the hemispheres.

Gender

The most prominent gender difference in the laterality of FCD occurred in the superior temporal cortex where males had stronger rightward lateralization of short- and long-range FCD than females. This finding is consistent with a stronger lateralization of superior temporal cortex functions in men than in women (Weekes et al. 1976). These gender differences could reflect testosterone levels during fetal development, which are higher for males than for females and can influence neural connectivity by averting programed cell death during neural development (De Vries and Simerley 2002). Thus, the more prominent rightward asymmetry in superior temporal and inferior frontal cortices for males than for females suggests a sexual dimorphism in brain lateralization. MRI studies have shown that toddlers with ASD had higher gray and white matter in the superior temporal cortex than controls, and this abnormal growth was more pronounced for females than for males (Schumann et al. 2010). Thus, the laterality patterns of the FCD could be used to test if ASD is an extreme of the typical male profile, as suggested by the extreme brain theory of autism (Baron-Cohen 2003), and could serve as a biomarker for ASD. On the other hand, the leftward lateralization of the long-range FCD in inferior frontal cortex was significantly stronger for females than for males, which suggests greater lateralization for the language function in the female brain. Some have proposed that the male brain is more asymmetrical than the female brain (Shaywitz et al. 1995), and our findings support an overall greater lateralization of short-range connectivity for males. However, this was not the case for the long-range connectivity for which there was higher asymmetry in some regions for females (inferior frontal) and in others for males (superior temporal). Note that a more widespread pattern of gender differences in laterality may emerge in nonresting conditions (i.e., during cognitive, emotional, or perceptual stimulation tasks).

Limitations

The 1000 functional connectomes database includes limited phenotypic characterization of the individuals. Thus, it was not possible to ascertain the functional significance of the gender effects on short- or long-range FCD. Nonetheless, the consistency of the findings from resting-state FCD patterns (Tomasi and Volkow 2010) makes it possible to generate standards that can be used in subsequent studies to compare with patient populations.

Conclusion

The FCD patterns showed a rightward asymmetry in temporal (short- and long-range) and cingulate cortices (long-range) and a leftward asymmetry in posterior occipital (short- and long-range) and inferior frontal (long-range) cortices and angular gyrus (long-range). The male brain was more rightward lateralized than the female brain. The lateralization of short-range connectivity was stronger for males than for females (rightward lateralized), whereas lateralization of long-range connectivity was stronger in some regions for females (leftward) and in others for males (rightward).

Funding

National Institutes of Alcohol Abuse and Alcoholism (2RO1AA09481).

Notes

Conflict of Interest : None declared.

References

Amunts K, Schleicher A, Bürgel U, Mohlberg H, Uylings HB, Zilles K. 1999. Broca's region revisited: cytoarchitecture and intersubject variability. J Comp Neurol. 412:319–341.

Anderson JS, Druzgal TJ, Froehlich A, Dubray MB, Lange N, Alexander AL, Abildskov T, Nielsen JA, Cariello AN, Cooperrider JR, et al. 2011. Decreased interhemispheric functional connectivity in autism. Cereb Cortex. 21:1134–1146.

Baron-Cohen S. 2003. The essential difference: men, women and the extreme male brain. London: Penguin.

Baron-Cohen S, Knickmeyer RC, Belmonte MK. 2005. Sex differences in the brain: implications for explaining autism. Science. 310: 819–823.

Barttfeld P, Wicker B, Cukier S, Navarta S, Lew S, Sigman M. 2011. A big-world network in ASD: dynamical connectivity analysis reflects a deficit in long-range connections and an excess of short-range connections. Neuropsychologia. 49:254–263.

Bassett DS, Bullmore E. 2006. Small-world brain networks. Neuroscientist. 12:512–523.

Bear D, Schiff D, Saver J, Greenberg M, Freeman R. 1986. Quantitative analysis of cerebral asymmetries. Fronto-occipital correlation, sexual dimorphism and association with handedness. Arch Neurol. 43:598–603.

Bilder RM, Wu H, Bogerts B, Ashtari M, Robinson D, Woerner M, Lieberman JA, Degreef G. 1999. Cerebral volume asymmetries in schizophrenia and mood disorders: a quantitative magnetic resonance imaging study. Int J Psychophysiol. 34:197–205.

Biswal B, DeYoe AE, Hyde JS. 1996. Reduction of physiological fluctuations in fMRI using digital filters. Magn Reson Med. 35:107–113.

Biswal B, Yetkin FZ, Haughton VM, Hyde JS. 1995. Functional connectivity in the motor cortex of resting human brain using echo-planar MRI. Magn Reson Med. 34:537–541.

Biswal BB, Mennes M, Zuo XN, Gohel S, Kelly C, Smith SM, Beckmann CF, Adelstein JS, Buckner RL, Colcombe S, et al. 2010. Toward discovery science of human brain function. Proc Natl Acad Sci U S A. 107:4734–4739.

Bressler SL. 1995. Large-scale cortical networks and cognition. Brain Res Rev. 20:288–304.

Bullmore E, Sporns O. 2009. Complex brain networks: graph theoretical analysis of structural and functional systems. Nat Rev Neurosci. 10:186–198.
Chance SA, Casanova MF, Switala AE, Crow TJ. 2008. Auditory cortex asymmetry, altered minicolumn spacing and absence of ageing effects in schizophrenia. Brain. 131:3178–3192.
Chance SA, Esiri MM, Crow TJ. 2005. Macroscopic brain asymmetry is changed along the antero-posterior axis in schizophrenia. Schizophr Res. 74:163–170.
Clements AM, Rimrodt SL, Abel JR, Blankner JG, Mostofsky SH, Pekar JJ, Denckla MB, Cutting LE. 2006. Sex differences in cerebral laterality of language and visuospatial processing. Brain Lang. 98:150–158.
Cordes D, Haughton VM, Arfanakis K, Carew JD, Turski PA, Moritz CH, Quigley MA, Meyerand ME. 2001. Frequencies contributing to functional connectivity in the cerebral cortex in "resting-state" data. AJNR Am J Neuroradiol. 22:1326–1333.
Crow TJ, Ball J, Bloom SR, Brown R, Bruton CJ, Colter N, Frith CD, Johnstone EC, Owens DG, Roberts GW. 1989. Schizophrenia as an anomaly of development of cerebral asymmetry. A postmortem study and a proposal concerning the genetic basis of the disease. Arch Gen Psychiatry. 46:1145–1150.
Devlin JT, Raley J, Tunbridge E, Lanary K, Floyer-Lea A, Narain C, Cohen I, Behrens T, Jezzard P, Matthews PM, et al. 2003. Functional asymmetry for auditory processing in human primary auditory cortex. J Neurosci. 23:11516–11522.
De Vries G, Simerley RB. 2002. Anatomy, development, and function of sexually dimorphic neural circuits in the mammalian brain. In: Pfaff DW, Arnold AP, Etgen AM, Fahrbach SE, Rubin RT, editors. Hormones, brain and behaviour: development of hormone-dependent neuronal systems. San Diego (CA): Academic Press. p. 137.
Falzi G, Perrone P, Vignolo L. 1982. Right-left asymmetry in anterior speech region. Arch Neurol. 39:239–240.
Foerster B, Tomasi D, Caparelli EC. 2005. Magnetic field shift due to mechanical vibration in functional magnetic resonance imaging. Magn Reson Med. 54:1261–1267.
Frost JA, Binder JR, Springer JA, Hammeke TA, Bellgowan PS, Rao SM, Cox RW. 1999. Language processing is strongly left lateralized in both sexes. Evidence from functional MRI. Brain. 122:199–208.
Galaburda AM. 1995. Anatomic basis of cerebral dominance. In: Davidson RJ, Hugdahl K, editors. Brain asymmetry. Cambridge (MA): MIT Press. p. 51–73.
Galaburda AM, LeMay M, Kemper TL, Geschwind N. 1978. Right-left asymmetrics in the brain. Science. 199:852–856.
Hirnstein M, Hausmann M, Lewald J. 2007. Functional cerebral asymmetry in auditory motion perception. Laterality. 12:87–99.
Huster RJ, Westerhausen R, Kreuder F, Schweiger E, Wittling W. 2007. Morphologic asymmetry of the human anterior cingulate cortex. Neuroimage. 34:888–895.
Hynd GW, Semrud-Clikeman M, Lorys AR, Novey ES, Eliopulos D. 1990. Brain morphology in developmental dyslexia and attention deficit-hyperactivity disorder (ADHD): morphometric analysis of MRI. Arch Neurol. 47:919–926.
Kertesz A, Black SE, Polk M, Howell J. 1986. Cerebral asymmetries on magnetic resonance imaging. Cortex. 22:117–127.
Larsen JP, Hoien T, Lundberg I, Odegaard H. 1990. MRI evaluation of the size and symmetry of the planum temporale in adolescents with developmental dyslexia. Brain Lang. 39:289–301.
LeMay M. 1976. Morphological cerebral asymmetries of modern man, fossil man, and nonhuman primate. Ann N Y Acad Sci. 280: 349–366.
LeMay M, Kido DK. 1978. Asymmetries of the cerebral hemispheres on computed tomograms. J Comput Assist Tomogr. 2:471–476.
Liu H, Stufflebeam SM, Sepulcre J, Hedden T, Buckner RL. 2009. Evidence from intrinsic activity that asymmetry of the human brain is controlled by multiple factors. Proc Natl Acad Sci U S A. 106:20499–20503.
Narr KL, Thompson PM, Sharma T, Moussai J, Zoumalan C, Rayman J, Toga AW. 2001. Three-dimensional mapping of gyral shape and cortical surface asymmetries in schizophrenia: gender effects. Am J Psychiatry. 158:244–255.
Okamoto H, Stracke H, Draganova R, Pantev C. 2009. Hemispheric asymmetry of auditory evoked fields elicited by spectral versus temporal stimulus change. Cereb Cortex. 19:2290–2297.
Paus T, Tomaiuolo F, Otaky N, MacDonald D, Petrides M, Atlas J, Morris R, Evans AC. 1996. Human cingulate and paracingulate sulci: pattern, variability, asymmetry, and probabilistic map. Cereb Cortex. 6:207–214.
Price CJ. 2010. The anatomy of language: a review of 100 fMRI studies published in 2009. Ann N Y Acad Sci. 1191:62–88.
Proust-Lima C, Amieva H, Letenneur L, Orgogozo JM, Jacqmin-Gadda H, Dartigues JF. 2008. Gender and education impact on brain aging: a general cognitive factor approach. Psychol Aging. 23:608–620.
Rubinov M, Sporns O. 2010. Complex network measures of brain connectivity: uses and interpretations. Neuroimage. 52:1059–1069.
Saugstad LF. 1999. A lack of cerebral lateralization in schizophrenia is within the normal variation in brain maturation but indicates late, slow maturation. Schizophr Res. 39:183–196.
Schönwiesner M, Krumbholz K, Rübsamen R, Fink GR, von Cramon DY. 2007. Hemispheric asymmetry for auditory processing in the human auditory brain stem, thalamus, and cortex. Cereb Cortex. 17:492–499.
Schroeder CE, Lakatos P. 2009. Low-frequency neuronal oscillations as instruments of sensory selection. Trends Neurosci. 32:9–18.
Schumann CM, Bloss CS, Barnes CC, Wideman GM, Carper RA, Akshoomoff N, Pierce K, Hagler D, Schork N, Lord C, et al. 2010. Longitudinal magnetic resonance imaging study of cortical development through early childhood in autism. J Neurosci. 30:4419–4427.
Sepulcre J, Liu H, Talukdar T, Martincorena I, Yeo BT, Buckner RL. 2010. The organization of local and distant functional connectivity in the human brain. PLoS Comput Biol. 6:e1000808.
Shaywitz BA, Shaywitz SE, Pugh KR, Constable RT, Skudlarski P, Fulbright RK, Bronen RA, Fletcher JM, Shankweiler DP, Katz L, et al. 1995. Sex differences in the functional organization of the brain for language. Nature. 373:607–609.
Steinmetz H. 1996. Structure, function and cerebral asymmetry: in vivo morphometry of the planum temporale. Neurosci Biobehav Rev. 20:587–591.
Takahashi T, Kawasaki Y, Kurokawa K, Hagino H, Nohara S, Yamashita I, Nakamura K, Murata M, Matsui M, Suzuki M, et al. 2002. Lack of normal structural asymmetry of the anterior cingulate gyrus in female patients with schizophrenia: a volumetric magnetic resonance imaging study. Schizophr Res. 55:69–81.
Toga AW, Thompson PM. 2003. Mapping brain asymmetry. Nat Rev Neurosci. 4:37–48.
Tomasi D, Caparelli EC, Chang L, Ernst T. 2005. fMRI-acoustic noise alters brain activation during working memory tasks. Neuroimage. 27:377–386.
Tomasi D, Volkow ND. 2010. Functional connectivity density mapping. Proc Natl Acad Sci U S A. 107:9885–9890.
Tomasi D, Volkow ND. Forthcoming 2011a. Aging and functional brain networks. Mol Psychiatry. doi:10.1038/mp.2011.81.
Tomasi D, Volkow ND. 2011b. Association between functional connectivity hubs and brain networks. Cereb Cortex. doi: 10.1093/cercor/bhq1268.
Tomasi D, Volkow ND. 2011c. Functional connectivity hubs in the human brain. Neuroimage. 57:908–917.
Tomasi D, Volkow ND. 2011d. Gender differences in brain functional connectivity density. Hum Brain Mapp. doi: 10.1002/hbm.21252.
Van Essen DC. 2005. A population-average, landmark- and surface-based (PALS) atlas of human cerebral cortex. Neuroimage. 28:635–662.
Weekes NY, Zaidel DW, Zaidel E. 1976. The effects of sex and sex role attribution on the right ear advantage in dichotic listening. Neuropsychology. 9:62–67.
Yan H, Zuo XN, Wang D, Wang J, Zhu C, Milham MP, Zhang D, Zang Y. 2009. Hemispheric asymmetry in cognitive division of anterior cingulate cortex: a resting-state functional connectivity study. Neuroimage. 47:1579–1589.
Yeni-Komshian GH, Benson DA. 1976. Anatomical study of cerebral asymmetry in humans, chimpanzees and rhesus monkeys. Science. 192:387–389.